Cellulose (2014) 21:1813–1821
DOI 10.1007/s10570-014-0207-5

ORIGINAL PAPER

Cellulose extracted from rice husk as filler for poly (lactic acid): preparation and characterization

Daniele Battegazzore · Sergio Bocchini · Jenny Alongi · Alberto Frache · Francesco Marino

Received: 16 December 2013 / Accepted: 17 February 2014 / Published online: 26 February 2014

Abstract The present manuscript has been focused on the extraction of cellulose from rice husk through a multi-step process. Three consecutive steps have been performed in order to separate impurities, hemicellulose, lignin and silica and thus to obtain pure cellulose. The crystallinity and morphology of the extracted cellulose have been investigated by using X-ray diffraction and scanning electron microscopy. Subsequently, poly(lactic acid) (PLA) bio-composites with different filler contents (namely, 5, 10, 20 and 30 wt%) have been prepared by melt-blending. The thermal and mechanical properties of the resulting bio-composites have been investigated and correlated with the observed morphologies. In spite of a broad micrometric distribution of the cellulose particle size, the mechanical properties turned out to be strongly improved as well as the oxygen permeability properties have proven to be reduced. These data have been compared with those of analogous compounds containing a commercial cellulose; the collected results have shown that similar mechanical properties have been found using both celluloses. Finally, this work has also demonstrated that an industrial waste as rice husk can be recycled for conferring enhanced final properties to PLA.

Keywords Cellulose · Rice husk · PLA · Mechanical properties · Oxygen permeability

D. Battegazzore (✉) · J. Alongi · A. Frache · F. Marino
Dipartimento di Scienza Applicata e Tecnologia, Politecnico di Torino, Sede di Alessandria, Viale Teresa Michel 5, 15121 Alessandria, Italy
e-mail: daniele.battegazzore@polito.it

S. Bocchini
Center for Space Human Robotics@PoliTo, Istituto Italiano di Tecnologia, C.so Trento 21, 10129 Turin, Italy

Introduction

Rice husk (RH) is an agricultural by-product material abundantly available in the world: Food and Agriculture Organization (FAO, report 2012) have estimated about 150 million tons in 2012. Indeed, RH has been already employed in different fields: as bio-fertilizer, as material for animal husbandry and absorbent material or pest control agent (Prasad and Pandey 2012). In addition, RH can be also used as a renewable fuel in cogenerating plants, considering its high calorific value (4,012 kcal/kg) (Tsai et al. 2007). Indeed, during its combustion, about 20–25 wt% of rice husk ash (RHA), containing more than 90 % silica with traces of other metal oxides, is produced (Patel et al. 1987). Such powder can be used as component in refractory bricks, as steel additive, as cement partial replacement (Prasad and Pandey 2012). In particular, Ashori et al. have investigated the effect of RHA as partial replacement of Portland cement (Torkaman et al. 2014) or as pozzolanic material (Hamzeh et al. 2013) or as filler for polymeric matrix (Nourbakhsh et al. 2011).

However, RH is often considered a waste product of the rice milling, and thus burned in air or dumped on wasteland. Therefore, many attempts have been carried out in order to find alternative and possible uses for RH, considering its abundance, composition and cheap cost. Indeed, RH is rich of cellulose (~40 %), hemicellulose (~30 %), lignin (~10 %) and silica (~20 %) (Hessien et al. 2009); hence, RH can be considered the most available cellulose source from agricultural crop residues in the world. As a consequence, several researchers have studied and optimized the extraction process of cellulose (Siró and Plackett 2010), also from RH (Johar et al. 2012) and rice straw (Lu and Hsieh 2012). Unfortunately, this material has not been yet employed for preparing bio-based composites by melt-blending, although many studies published in the literature have shown that cellulose may confer a general improvement of poly(lactic acid) properties (Battegazzore et al. 2013 and references quoted in, Kalia et al. 2011).

Thus, novelty of the present manuscript is the use of cellulose derived from RH for preparing bio-composites by melt-blending. In doing so, an industrial waste from the agricultural field has been recycled for conferring enhanced final properties to PLA. The achieved properties turned out to be comparable with those observed with a synthetic cellulose, but with the great advantage that in our study a waste has been recycled.

Experimental part

Materials

Poly(lactic acid)—PLA—(3251D grade, MFI = 80 g/10 min at 210 °C under 2.16 kg) was purchased from NatureWorks LLC, and rice husk as by-products was kindly supplied by S.P. S.p.A., respectively. H_2SO_4, KOH, $NaClO_2$ and CH_3COOH (reagent grade) were purchased from Sigma-Aldrich.

Extraction of cellulose from RH

In a typical experiment, 150 g of milled RH were placed in 1,000 g of distilled water and 39 g of H_2SO_4 under stirring at 90 °C for 2 h in order to hydrolyze hemicellulose and to remove impurities, as reported by Krishnarao et al. (2001). The solid residue was separated by filtration and purified in deionized water. Subsequently, in order to extract silica, such residue was further treated with 1,000 g of distilled water and 50 g of KOH under stirring at 90 °C for 2 h. Once again, the solid residue was filtrated and purified. During the third step, an aqueous solution of $NaClO_2$ (30 g in 1,000 g of water) was used in order to remove amorphous cellulose and lignin; the pH was arranged to 4.5, employing CH_3COOH. Then, the solution was heated at 75 °C and maintained under stirring for 4 h. The final residue was further washed with deionized water and dried to obtain 26 % of cellulose (C) yield. Figure 1 shows a schematic representation of the extraction procedure described above.

Preparation of PLA/cellulose-based bio-composites

PLA and cellulose were dried at 80 °C in a vacuum convection oven for 5 and 12 h respectively. Subsequently, PLA-based composites with different cellulose contents (namely, 5, 10, 20 and 30 wt%) were prepared by melt-blending, using a co-rotating twin screw micro extruder DSM Xplore 15 ml Microcompounder. Residence time was fixed at 5 min for all runs. To prevent PLA degradation, a N_2 purge flow was used during processing. The screw speed was fixed at 60 and 100 rpm for feed and melt mixing, respectively. Heating temperature was set at 180 °C. Hereafter, the samples have been coded on the basis of the nominal compositions: as an example, PLA5C refers to composite nominally loaded with 5 wt% of cellulose.

Pellets obtained by extrusion were dried at 80 °C for 6 h in a vacuum convection oven, before the preparation of suitable specimens for dynamic-mechanical thermal analysis (DMTA) and oxygen permeability tests (OP). These specimens ($60 \times 60 \times 1$ mm^3 and $100 \times 100 \times 0.2$ mm^3 for DMTA and OP, respectively) were prepared by using a hot compression molding press at 180 °C for 3 min (pressure of 5 MPa).

Characterization techniques

The chemical structure of RH and cellulose was evaluated by Attenuated Total Reflectance (ATR) coupled with infrared spectroscopy (FTIR). ATR spectra were recorded at room temperature in the range 4,000–600 cm^{-1} (16 scans and 4 cm^{-1}

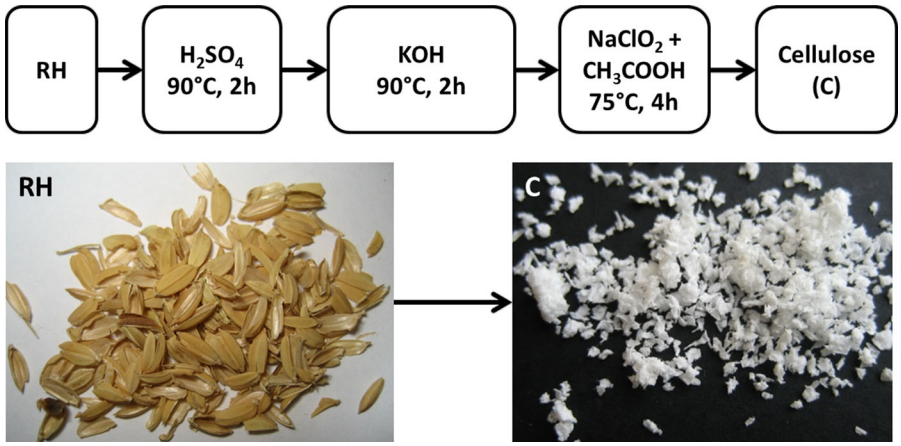

Fig. 1 Schematic representation of the cellulose extraction from RH

resolution), using a Perkin-Elmer Frontier FT-IR/FIR spectrophotometer, equipped with a diamond crystal.

X-ray diffraction (XRD) analyses were performed on 30 × 30 × 0.5 mm^3 samples with a Philips X'Pert-MPD diffractometer (Cu-K_α radiation, $k = 1.540562$ Å; step size: 0.02°; step time: 2 s).

The surface morphology of the extracted cellulose and prepared bio-composites was studied using a LEO-1450VP Scanning Electron Microscope—SEM—(beam voltage: 20 kV). The samples were obtained fracturing 1 mm thick films in liquid nitrogen (5 × 1 mm^2). These pieces were pinned up to conductive adhesive tapes and gold-metallized. Cellulose powder was metallized with gold, as well. The morphological observations were completed by optical microscopy (OM), using a Nikon Eclipse LV100D instrument in transmission mode.

Thermogravimetric Analysis (TGA) was performed placing samples (ca. 10 mg) in open alumina pans, by using a Q500 TA Instruments analyser, from 50 to 800 °C at 10 °C/min with a nitrogen or air flow of 60 ml/min.

Differential Scanning Calorimetry (DSC) analyses were performed on 8 mg samples using a Q20 TA Instruments analyser, with a double cycle of heating from 0 to 200 °C at 10 °C/min, separated by a single cooling cycle at 10 °C/min. The glass transition temperature (T_g), crystallization temperature (T_c), cold crystallization temperature (T_{cc}), melting temperature (T_m) and melting enthalpy (ΔH_m) were determined from the second heating scan. The crystallinity (χ) of PLA and bio-composites was evaluated following Eq. (1).

$$\chi = \left(\frac{\Delta H}{\Delta H_m^0 * \left(1 - \frac{\%wt\ filler}{100}\right)} \right) * 100 \quad (1)$$

where $\Delta H = \Delta H_m$ (from second heating scan), ΔH_m^0 is the melting enthalpy of a 100 % crystalline polymer matrix (93.0 J/g for PLA (Garlotta 2002 and Turner et al. 2004)) and *%wt filler* is the filler weight percentage.

DMTA were performed using a Q800 DMA (TA Instruments) with tension film clamp. The experimental conditions were set: temperature range of 30–120 °C, heating rate of 3 °C/min, 1 Hz of frequency, 0.05 % of deformation amplitude, strain-controlled mode. All tests were made according to the ISO 6721 standard.

The data collected by DMTA at 30 °C have been employed to fit the modulus experimental value of cellulose within PLA, using Voigt micro-mechanical model, following Eq. (2).

$$E_c = \phi_m E_m + \phi_f E_f \quad (2)$$

where E_c, E_m and E_f are composite, matrix and filler moduli, respectively, and ϕ_m and ϕ_f the corresponding volumetric fractions.

OP was measured at 23 °C and 65 % relative humidity, by using a Multiperm ExtraSolution instrument, with an initial conditioning time of 3 h. The end of the test was established when the collected data

reached an oxygen transmission rate (OTR) accuracy of 0.5 %. The OP was calculated following Eq. (3).

$$OTR = \frac{volume\ O_2}{area * day * pressure}$$
$$OP = OTR * film \text{ thickness} \quad (3)$$

Results and discussion

Characterization of cellulose

As mentioned above, cellulose has been extracted from RH through a multi-step process, and the resulting powder has been characterized from the chemical and morphological point of view, by using ATR-FTIR, XRD and SEM.

Infrared spectroscopy provides suitable information on the chemical structure of the original RH and extracted cellulose. Figure 2 shows the ATR spectra of RH and cellulose compared with that of a common absorbent cotton.

As far as RH is concerned, numerous peaks are visible (apart from the broad band of water between 3,750 and 2,800 cm^{-1}) attributable to its main components: hemicellulose (1,732 cm^{-1}), lignin (1,542 cm^{-1}) and silica (1,063 and 800 cm^{-1}). The typical vibrations of cellulose are hidden by the broad band at 1,063 cm^{-1}, as shown also by the shoulder located between 1,300 and 1,070 cm^{-1} (Socrates 2001).

When cellulose is extracted from RH, the characteristic bands of silica, hemicellulose and lignin disappear; only the cellulose vibrations are still detectable, as evidenced comparing the ATR spectra

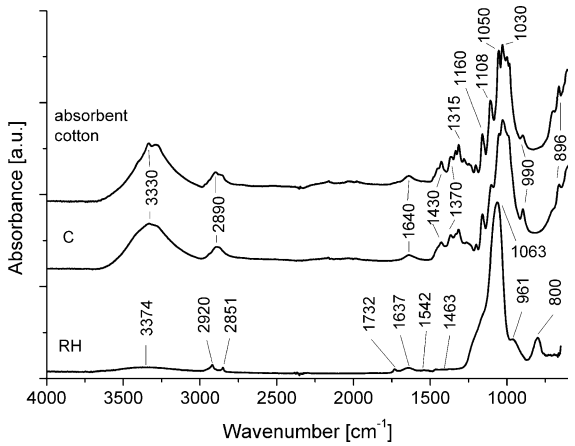

Fig. 2 ATR spectra of RH, cellulose (C) and absorbent cotton

of the extracted cellulose and absorbent cotton (namely, ν(OH) at 3,330, ν(CH_2) at 2,890, δ(OH) at 1,640, δ(CH_2) at 1,430, δ(CH) at 1,370 and 1,315, pyranose ring skeletal vibrations involving C–O and C–C groups at 1,160, 1,050, 1,030 and 896, δ(OH) at 990 cm^{-1}) (Johar et al. 2012).

Pursuing our research, the crystallinity and morphology of the extracted cellulose have been investigated by using XRD and SEM, respectively. Indeed, cellulose has a crystalline structure with respect to hemicellulose and lignin, which are amorphous in nature. More specifically, cellulose has a crystalline structure due to the hydrogen bond interactions and Van der Waals forces between adjacent macromolecules (Zhang and Lynd 2004).

Figure 3a reports the XRD pattern of the extracted cellulose; four main peaks have been found at ca. 16°, 17°, 22° and 34°. It is difficult to discriminate if the extracted cellulose can have a Iα or Iβ form: thus, 16°, 17°, 22° and 34° 2θ could be ascribed to either (100), (010), (110) and (11–4) or to (1–10), (110), (200) and (004) of the cellulose Iα or Iβ patterns, according to the literature (French 2013; Nishiyama et al. 2002 and 2003). However, it is reasonable to suppose that our cellulose has a Iβ crystalline form due to its natural origin, being derived from rice husk. Indeed, most plants contain cellulose in Iβ instead of Iα crystalline form.

As far as the morphology of cellulose is concerned, Fig. 3b shows that the extracted powder is characterized by the presence of regular fibers with a diameter ranging between 2 and 5 μm, having a broad distribution of lengths (from hundreds μm until several mm). In addition, some structures of bundled fibers are still detectable.

Characterization of PLA/cellulose-based biocomposites

Morphological analysis

The morphology of the prepared bio-composites has been investigated by optical and electron microscopies: in Fig. 4, two optical and two SEM magnifications of PLA loaded with 5 and 30 wt% are reported as examples (4a, b for PLA5C, 4c, d for PLA30C, respectively). The extracted cellulose exhibits a homogeneous distribution within the polymer matrix,

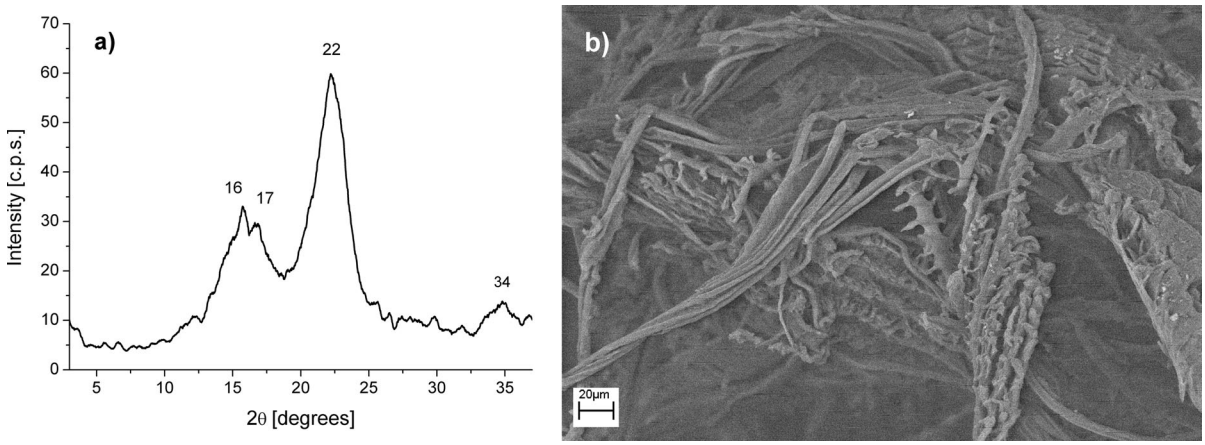

Fig. 3 XRD patterns (**a**) and SEM micrograph of the extracted cellulose (**b**)

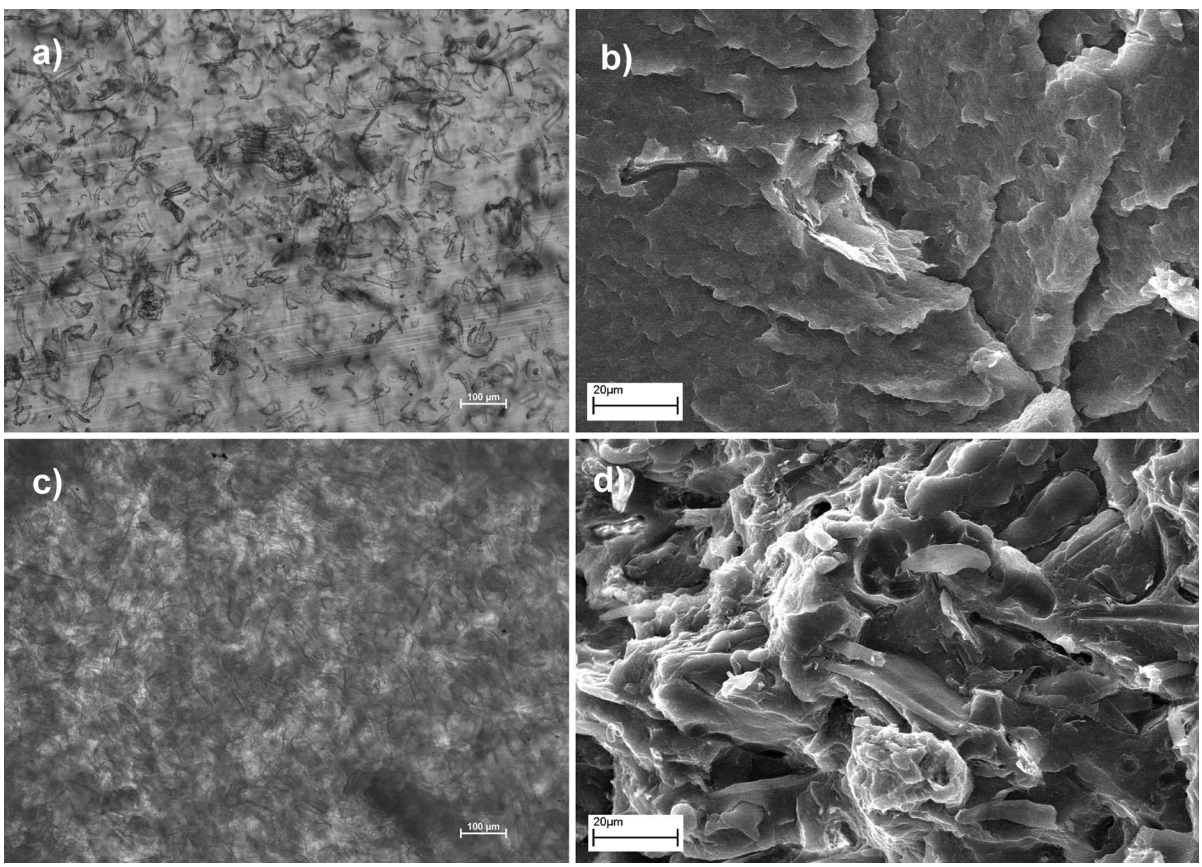

Fig. 4 Optical and SEM magnifications of PLA5C (**a** and **b**) and PLA30C (**c** and **d**)

regardless of its content and its broad micrometric distribution of particle size. In addition, a good adhesion between cellulose and PLA has been detected, also at highest filler content (namely, 30 wt%). Furthermore, optical microscopy has shown that the melt-blending process is capable to strongly

reduce the fiber length as well as to de-bundle them, favoring a finer dispersion.

Thermal properties

The thermal properties of the prepared bio-composites have been investigated and compared with those of pure PLA, by using TGA and DSC techniques.

The thermogravimetry have been mainly used to establish the effect of cellulose content on PLA thermal stability. Figure 5 reports the weight losses of cellulose-based bio-composites in nitrogen (5a) and air (5b), as a function of temperature (TG curves). The main thermal degradation mechanism of PLA involves the alcoholysis/acidolysis of polylactide ester groups (Bocchini and Camino 2012): these reactions lead to the formation of lactide and cyclic oligomers in the case of intramolecular arrangements, and to the formation of linear oligomers when intermolecular reactions occur.

The presence of cellulose does not significantly change the degradation mechanism of PLA in both atmospheres, with the exception of a slight anticipation. Indeed, cellulose may act as initiator due to the abundance of hydroxyl groups present in its structure that can react with PLA ester groups. Furthermore, it is noteworthy that the final residue of PLA in nitrogen increases due to the filler presence. Higher cellulose content, higher is the final residue in nitrogen. On the other hand, in air, taking into account the thermal degradation of pure cellulose, the curves of bio-composites are superimpositions of pure PLA and cellulose TG curves.

Table 1 DSC data of PLA and cellulose-based bio-composites

Sample	T_c (°C)	T_g (°C)	T_{cc} (°C)	T_m (°C)	ΔH_m (J/g)	χ (%)
PLA	–	61	–	–	–	–
PLA5C	–	61	130	154	16.1	18
PLA10C	–	61	127	154	21.3	25
PLA20C	–	61	124	153	21.7	29
PLA30C	–	61	118	151–156	20.3	31

The thermal analysis has been completed by DSC measurements: Table 1 reports the collected data. As already reported (Battegazzore et al. 2011; Fukushima et al. 2009a, b), a semi-crystalline PLA is characterized by an unusual thermal behavior due to the absence of crystallization during cooling, and the presence of cold crystallization during heating, as well as splitting of the melting temperature, sometimes.

Table 1 and Fig. 6 confirm that the addition of cellulose does not induce PLA crystallization during the cooling run (absence of T_c) and does not significantly affect its T_g. On the other hand, the presence of cellulose (regardless of its content) induces a cold crystallization phenomenon (*see* T_{cc} values), not observed in PLA, during heating run. In doing so, cellulose-based composites have shown a T_m, due to the melting of crystalline domains nucleated during cold crystallization. As a result, in the adopted experimental conditions, PLA composites have exhibited a certain crystallinity degree, that can be assessed following Eq. (1) (reported in the Experimental Part),

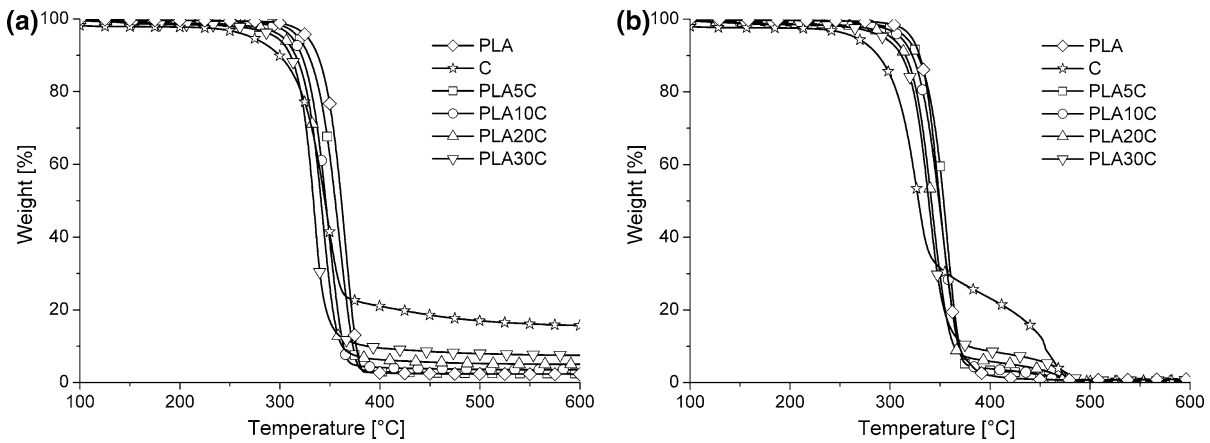

Fig. 5 TG curves of PLA and cellulose/PLA bio-composites in nitrogen (**a**) and air (**b**)

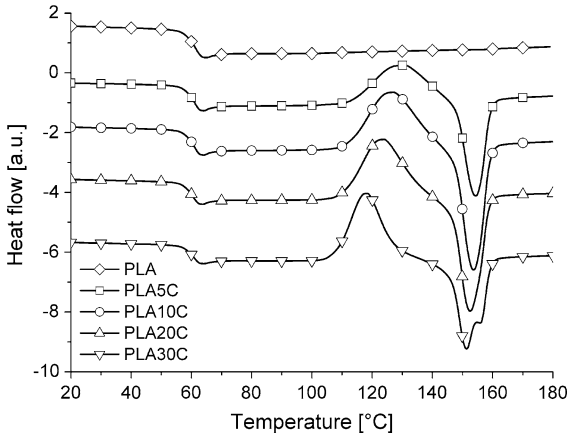

Fig. 6 DSC curves of PLA and cellulose-based bio-composites

and on the basis of the experimental values of ΔH_m collected by DSC measurements. It is important to highlight that the use of such equation is possible as cellulose does not give any phenomena overlapping with those of PLA in the adopted experimental conditions.

From an overall consideration, higher cellulose content, higher is the crystallinity of PLA compounds. However, the amount of crystallinity developed in PLA is strongly dependent on the cooling rate of the melt.

Mechanical properties

The mechanical properties of the prepared bio-composites have been thoroughly investigated in order to evaluate the effect of filler content on PLA storage modulus in 30–120 °C range. In addition, the data collected by DMTA at 30 °C have been employed to fit the experimental value of cellulose modulus within PLA, using Voigt micro-mechanical model. Figure 7a reports the trend of the storage modulus (E') as a function of temperature and Table 2 summarizes the collected data.

A general increase of E' has been registered for all bio-composites (Fig. 7a), revealing that the filler modulus could be higher than that of PLA (Table 2), as expected. It is noteworthy that bio-composites exhibit higher storage moduli than that of pure PLA at high temperatures (>100 °C), in accordance with the percentage crystallinity increase found by DSC (Table 1). For pure PLA and bio-composites, the mechanical property collapse occurs at about 70 °C, estimated as maximum of tanδ curve.

Pursuing our research, the assessment of cellulose density and modulus has been carried out. To this aim, Archimede's law has been exploited (performing weight measurements in air and water): a value of 1.48 and 1.25 g/cm^3 has been found for cellulose and pure PLA, respectively. Subsequently, the density values already found have been used for calculating the volumetric fractions (ϕ) required by Voigt micro-mechanical model (Eq. 2). Indeed, such model can be a useful tool for assessing the modulus of natural fillers, like cellulose, as previously described (Battegazzore et al. 2013). As result, E_f value (calculated

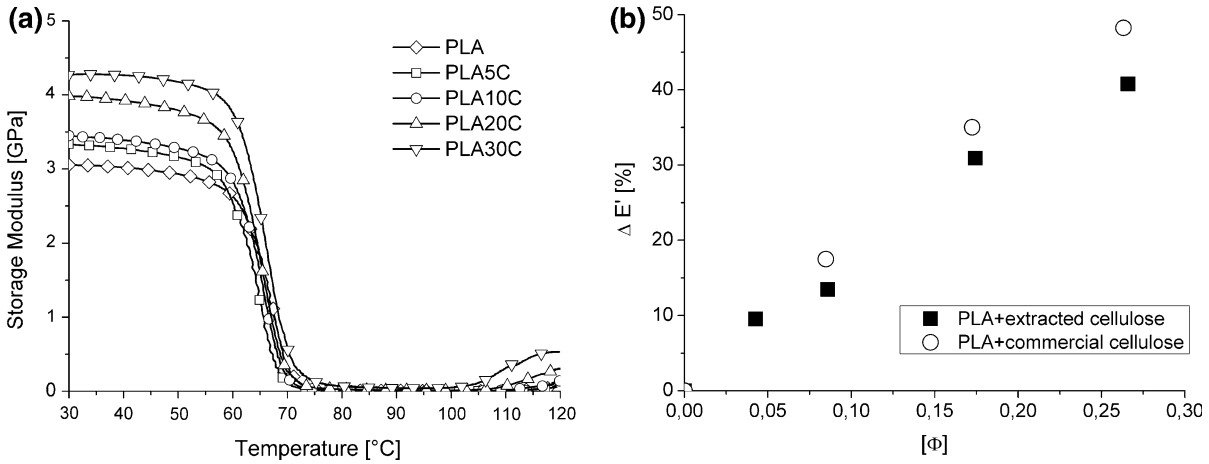

Fig. 7 Storage modulus of PLA and cellulose-based bio-composites (**a**) and modulus percent increase as a function of cellulose content (**b**)

Table 2 Storage modulus and percent increase of PLA and cellulose-based bio-composites

Sample		PLA	PLA5C	PLA10C	PLA20C	PLA30C
E′ at 30 °C	(MPa)	3,050	3,330	3,450	3,980	4,280
ΔE′*	(%)	–	+10	+13	+31	+41

$*\Delta E' = \left(E'_{PLA} - E'_{bio-composite}\right)/E'_{PLA}$

using E_m and E_c data from DMTA) was 8.0 GPa with a maximum punctual error of 2.4 %.

In order to establish if the extracted cellulose exhibits the same behavior of other celluloses in terms of property improvements, the collected mechanical data have been compared with those previously published (Battegazzore et al. 2013), employing a commercial cellulose. Figure 7b reports modulus percent increase as a function of cellulose content for both data. It is noteworthy that similar percent improvements of the storage modulus have been achieved employing both celluloses, at the same content. It is reasonable that similar matrix/filler interactions occur in both cases, regardless of cellulose origin. Indeed, comparable aspect ratios (namely, surface area and length) and adhesion levels have been observed during the morphological analysis by SEM.

Oxygen barrier properties

The oxygen barrier properties of the prepared bio-composites have been tested: Table 3 lists these data, where the permeability (OP) was calculated following the Eq. (3).

The collected data show that the oxygen permeability of PLA is significantly affected by the presence of cellulose and that OP decreases by cellulose content increase. Such reduction may be partially due to the good adhesion between filler and matrix as well as to the homogeneous distribution of filler within polymer matrix (observed by optical microscopy and SEM, Fig. 4). Indeed, the presence of cellulose can create a tortuous path that slows down the progress of gas molecules through the polymer matrix. This phenomenon can be ascribed to both the presence of cellulose chains and to the crystalline domains induced and favored by the filler. By this way, the bio-composites turned out to be less permeable to the oxygen diffusion with respect to neat PLA. Finally, it is important to highlight that the permeability features of cellulose-based composites is affected by the crystallinity of the tested film. Indeed, this latter cannot be considered the same assessed by DSC, as the specimens for OP test were prepared by compression molding, during which the cooling rate is not so strictly controlled as well as in the DSC experiments.

Table 3 Oxygen permeability of PLA and cellulose-based bio-composites

Sample	Thickness (mm)	OTR [cc/(m^2 bar 24 h)]	OP [cc mm/(m^2 bar 24 h)]	δ* (%)
PLA	0.185	86	15.9	–
PLA5C	0.205	63	12.9	−19
PLA10C	0.205	55	11.2	−29
PLA20C	0.215	42	9.1	−43
PLA30C	0.195	37	7.2	−55

$*\delta = \left(OP_{bio-composite} - OP_{PLA}\right)/OP_{PLA}$

Conclusions

In the present study, bio-composites consisting of poly(lactic acid) and cellulose derived from rice husk have been prepared by melt-blending. The effect of different filler contents has been investigated on the thermal, mechanical and oxygen barrier properties of PLA. The collected data by DMTA have shown that the presence of cellulose has induced a significant improvement of the mechanical properties (depending on filler content) as well as a slight reduction of the oxygen permeability of PLA.

The most interesting aspect of this work is that similar mechanical and oxygen permeability properties have been achieved (without affecting the thermal stability of PLA), employing both commercial cellulose and cellulose derived from rice husk; but above all, an industrial waste has been recycled for conferring enhanced final properties to PLA. Indeed, as already mentioned, rice husk is often considered a

waste product of the rice milling, and thus burned in air or dumped on wasteland.

Acknowledgments The authors would like to thank FONDO EUROPEO DI SVILUPPO REGIONALE (P.O.R. 2007–2013) and FONDO EUROPEO AGRICOLO PER LO SVILUPPO RURALE (P.S.R. 2007–2013) sponsor of ECOFOOD project.

References

Battegazzore D, Bocchini S, Frache A (2011) Crystallization kinetics of poly(lactic acid)-talc composites. Express Polym Lett 5(10):849–858. doi:10.3144/expresspolymlett.2011.84

Battegazzore D, Alongi J, Frache A (2013) Poly(lactic acid)-based composites containing natural fillers: thermal, mechanical and barrier properties. J Polym Environ. doi:10.1007/s10924-013-0616-9

Bocchini S, Camino G (2012) Flammability and thermal stability in clay/polyesters nano-biocomposites. Green Energy Technol 50:265–285. doi:10.1007/978-1-4471-4108-2

FAO Rice Market Monitor (2012) Vol. XV—issue no. 4; November 2012

French AD (2013) Idealized powder diffraction patterns for cellulose polymorphs. Cellulose. doi:10.1007/s10570-013-0030-4

Fukushima K, Abbate C, Tabuani D, Gennari M, Camino G (2009a) Biodegradation of poly (lactic acid) and its nanocomposites. Polym Degrad Stab 94(10):1646–1655. doi:10.1016/j.polymdegradstab.2009.07.001

Fukushima K, Tabuani D, Camino G (2009b) Nanocomposites of PLA and PCL based on montmorillonite and sepiolite. Mater Sci Eng, C 29(4):1433–1441. doi:10.1016/j.msec.2008.11.005

Garlotta D (2002) A literature review of poly (lactic acid). J Polym Environ 9(2):63–84. doi:10.1023/A:1020200822435

Hamzeh Y, Pourhooshyar K, Torkaman J, Ashori A, Jafari M (2013) Study on the effects of white rice husk ash and fibrous materials additions on some properties of fiber e cement composites. J Environ Manag 117:263–267. doi:10.1016/j.jenvman.2013.01.002

Hessien MM, Rashad MM, Zaky RR, Abdel-Aal EA, El-Barawy KA (2009) Controlling the synthesis conditions for silica nanosphere from semi-burned rice straw. Mater Sci Eng, B 162(1):14–21. doi:10.1016/j.mseb.2009.01.029

Johar N, Ahmad I, Dufresne A (2012) Extraction, preparation and characterization of cellulose fibres and nanocrystals from rice husk. Ind Crops Prod 37(1):93–99. doi:10.1016/j.indcrop.2011.12.016

Kalia S, Dufresne A, Cherian BM, Kaith BS, Avérous L, Njuguna J, Nassiopoulos E (2011) Cellulose-based bio- and nanocomposites: a review. Int J Polym Sci 2011:1–35. doi:10.1155/2011/837875

Krishnarao RV, Subrahmanyam J, Jagadish Kumar T (2001) Studies on the formation of black particles in rice husk silica ash. J Eur Ceram Soc 21(1):99–104. doi:10.1016/S0955-2219(00)00170-9

Lu P, Hsieh YL (2012) Preparation and characterization of cellulose nanocrystals from rice straw. Carbohydr Polym 87(1):564–573. doi:10.1016/j.carbpol.2011.08.022

Nishiyama Y, Langan P, Chanzy H (2002) Crystal structure and hydrogen-bonding system in cellulose Iβ from synchrotron X-ray and neutron fiber diffraction. J Am Chem Soc 124:9074–9082. doi:10.1021/ja0257319

Nishiyama Y, Sugiyama J, Chanzy H, Langan P (2003) Crystal structure and hydrogen bonding system in cellulose I(alpha) from synchrotron X-ray and neutron fiber diffraction. J Am Chem Soc 125(47):14300–14306. doi:10.1021/ja037055w

Nourbakhsh A, Farhani F, Ashori A (2011) Nano-SiO_2 filled rice husk/polypropylene composites: physico-mechanical properties. Ind Crops Prod 33(1):183–187. doi:10.1016/j.indcrop.2010.10.010

Patel M, Karera A, Prasanna P (1987) Effect of thermal and chemical treatments on carbon and silica contents in rice husk. J Mater Sci 22(7):2457–2464. doi:10.1007/BF01082130

Prasad R, Pandey M (2012) Rice husk ash as a renewable source for the production of value added silica gel and its application: an overview. Bull Chem React Eng Catal 7(1):1–25. doi:10.9767/bcrec.7.1.1216.1-25

Siró I, Plackett D (2010) Microfibrillated cellulose and new nanocomposite materials: a review. Cellulose 17(3):459–494. doi:10.1007/s10570-010-9405-y

Socrates G (2001) Infrared and Raman characteristic group frequencies: tables and charts. Wiley, Chichester

Torkaman J, Ashori A, Sadr Momtazi A (2014) Using wood fiber waste, rice husk ash, and limestone powder waste as cement replacement materials for lightweight concrete blocks. Constr Build Mater 50:432–436. doi:10.1016/j.conbuildmat.2013.09.044

Tsai WT, Lee MK, Chang YM (2007) Fast pyrolysis of rice husk: product yields and compositions. Bioresour Technol 98(1):22–28. doi:10.1016/j.biortech.2005.12.005

Turner JF, Riga A, O'Connor A, Zhang J, Collis J (2004) Characterization of drawn and undrawn poly-L-lactide films by differential scanning calorimetry. J Therm Anal Calorim 75(1):257–268. doi:10.1023/B:JTAN.0000017347.08469.b1

Zhang YP, Lynd LR (2004) Toward an aggregated understanding of enzymatic hydrolysis of cellulose: noncomplexed cellulose system. Biotechnol Bioeng 88:797–824. doi:10.1002/bit.20282